

---

# TRUE: A Trustworthy Unified Explanation Framework for Large Language Model Reasoning

---

Yujiao Yang

Dalian University of Technology  
Dalian, China  
yjyang@mail.dlut.edu.cn

## Abstract

Large language models (LLMs) have demonstrated strong capabilities in complex reasoning tasks, yet their decision-making processes remain difficult to interpret. Existing explanation methods often lack trustworthy structural insight and are limited to single-instance analysis, failing to reveal reasoning stability and systematic failure mechanisms. To address these limitations, we propose the Trustworthy Unified Explanation Framework (TRUE), which integrates executable reasoning verification, feasible-region directed acyclic graph (DAG) modeling, and causal failure mode analysis. At the instance level, we redefine reasoning traces as executable process specifications and introduce blind execution verification to assess operational validity. At the local structural level, we construct feasible-region DAGs via structure-consistent perturbations, enabling explicit characterization of reasoning stability and the executable region in the local input space. At the class level, we introduce a causal failure mode analysis method that identifies recurring structural failure patterns and quantifies their causal influence using Shapley values. Extensive experiments across multiple reasoning benchmarks demonstrate that the proposed framework provides multi-level, verifiable explanations, including executable reasoning structures for individual instances, feasible-region representations for neighboring inputs, and interpretable failure modes with quantified importance at the class level. These results establish a unified and principled paradigm for improving the interpretability and reliability of LLM reasoning systems.

## 1 Introduction

Large language models (LLMs) have demonstrated remarkable capabilities across a wide range of complex reasoning tasks, including mathematical problem solving, logical inference, and knowledge-intensive decision-making. Understanding how LLMs arrive at their decisions is crucial not only for revealing the boundaries of their reasoning capabilities, but also for improving human trust in model behavior, thereby enabling more reliable optimization and safer deployment Lanham et al. [2023], Paul et al. [2024]. Consequently, explaining the decision-making mechanisms of LLMs and characterizing their reasoning behavior has become a central problem in contemporary LLM research Tutek et al. [2025].

However, due to the massive scale of training data and model parameters, as well as the highly complex internal structure of LLMs, traditional explanation methods—such as perturbation-based or attention-based attribution techniques—often fail to provide explanations with meaningful structural insight Agarwal et al. [2024]. More recent approaches attempt to improve interpretability by prompting LLMs to generate step-by-step reasoning processes Cahlik et al. [2025]. While prompting-based explanations can enhance predictive performance and provide intuitive reasoning traces, prior studies show that these explanations often constitute post-hoc rationalizations rather than faithful representations of the model’s true decision-making process Turpin et al. [2023], Barez et al. [2025].

Furthermore, existing local explanation methods typically focus on individual instances in isolation, ignoring reasoning structures shared across related inputs and failing to reveal systematic behavioral patterns or structural failure mechanisms at the problem-class level.

To address these limitations, we propose a novel composite explanation framework for LLMs. The proposed framework extends the scope of explanation from single-instance reasoning traces to structured reasoning representations at the local group level, enabling a unified explanation paradigm that spans instance-level and class-level reasoning behavior. This shift elevates explanations from descriptive textual artifacts to verifiable, executable, and structurally grounded representations of reasoning processes. Specifically, we first redefine explanations as executable reasoning specifications, and introduce an independent executor that attempts to recover the final answer solely from the explanation steps. This protocol directly verifies whether the explanation encodes a complete and operational solution procedure, thereby establishing a verifiable link between explanation executability and reasoning correctness at the single-instance level.

Building upon this executable foundation, the framework further explores the local input neighborhood through structure-preserving perturbations and constructs a reasoning trajectory Directed Acyclic Graph (DAG) to represent the local feasible region. This structural representation enables explicit modeling of the stability and executability of reasoning processes across semantically similar inputs. Furthermore, by aggregating reasoning structures over clusters of semantically related samples and introducing controlled counterfactual perturbations, the framework identifies and quantifies recurring structural failure modes at the class level. This analysis reveals systematic behavioral patterns and underlying structural limitations of LLM reasoning across problem categories. Through this multi-level structural formulation, the proposed framework validates individual reasoning processes and enables systematic characterization of reasoning stability and failure mechanisms.

We conduct extensive experiments on multiple representative reasoning benchmarks to evaluate the effectiveness of the proposed framework across different structural levels. The results show that executable explanations reliably capture the validity of reasoning structures at the instance level; local feasible-region modeling effectively characterizes the structural stability of reasoning behavior; and cluster-level failure mode analysis identifies interpretable and quantifiable systematic reasoning deficiencies at the class level. Collectively, these findings demonstrate that the proposed framework provides a unified structural approach for explaining and diagnosing LLM reasoning behavior, offering a principled interpretability perspective for understanding LLM reasoning mechanisms and their inherent limitations.

## 2 Related Works

### 2.1 Perturbation-Based Local Explanation Methods

Perturbation-based local explanation methods estimate input importance by applying controlled modifications to the input and observing the resulting changes in model outputs. These approaches characterize model behavior within the local neighborhood of individual instances and constitute one of the most widely used model-agnostic explanation paradigms Ribeiro et al. [2016]. This paradigm has been extended to large language models (LLMs), where tokens, context segments, or prompts are selectively removed, replaced, or modified to analyze their influence on model predictions Turpin et al. [2023], Madani et al. [2025], Ortu et al. [2024]. Such perturbation-based analyses have been widely employed to investigate in-context learning mechanisms, prompt sensitivity, and the stability of model reasoning.

Among perturbation-based approaches, Shapley-value-based methods provide a theoretically grounded framework for attribution by quantifying the marginal contribution of input components Lundberg and Lee [2017]. Recent extensions adapt Shapley-based attribution to LLMs for token-level and context-level explanation, such as TokenSHAP Horovicz and Goldshmidt [2024], Xiao et al. [2025] and context attribution methods Liu et al. [2024], Patel et al. [2025]. Related work also applies Shapley-based data attribution to analyze the influence of training data or in-context examples on model behavior Tan et al. [2025], Naudot et al. [2025]. Despite their theoretical rigor, these methods are computationally expensive and capture correlations between inputs and predictions.

Overall, perturbation-based methods focus on identifying influential input components but do not explicitly model the structural organization of reasoning processes. Consequently, they cannot

verify whether explanations constitute complete and executable reasoning procedures, nor can they characterize reasoning stability across related inputs or identify structural failure modes.

## 2.2 Prompting-Based Explanation Methods

Prompting-based explanation methods leverage the reasoning capabilities of large language models (LLMs) to generate intermediate reasoning steps, providing explanations in the form of natural language reasoning traces. A representative example is Chain-of-Thought (CoT) prompting Wei et al. [2022], which induces models to explicitly generate step-by-step reasoning, making their decision process observable and analyzable. Subsequent extensions, including Zero-Shot CoT Kojima et al. [2022], Plan-and-Solve prompting Wang et al. [2023], and Self-Refine Madaan et al. [2023], further demonstrate that structured prompting can reliably elicit coherent and interpretable reasoning traces, providing a practical approach for examining model reasoning behavior.

Several studies have analyzed prompting-based explanations to understand how reasoning traces reflect model behavior. For example, modifying demonstrations or introducing contradictory input-label mappings reveals that large models can flexibly adapt their reasoning processes, indicating structured reasoning capabilities beyond memorized priors Han et al. [2023], Wei et al. [2023]. Other work applies perturbation and attribution techniques to CoT reasoning traces, showing that intermediate reasoning steps influence prediction stability and guide the generation process Wang et al. [2022], Chuang et al. [2025]. Counterfactual prompting further demonstrates that reasoning traces play a functional role in shaping model outputs Madaan et al. [2022], Zhou et al. [2023].

However, some studies have raised concerns regarding the faithfulness of prompting-based explanations. Generated reasoning traces may act as post-hoc rationalizations correlated with predictions rather than faithfully reflecting the true decision process Turpin et al. [2023], Lanham et al. [2023]. Models can produce plausible reasoning even when predictions are incorrect or driven by spurious correlations, suggesting that textual reasoning traces alone may not reliably capture the underlying reasoning mechanisms.

Overall, prompting-based explanation methods provide interpretable reasoning traces that improve transparency of model behavior. However, these approaches typically treat explanations as descriptive text without verifying whether they constitute complete and executable reasoning procedures. Moreover, they primarily operate at the single-instance level and do not model shared reasoning structures across related inputs or identify systematic failure modes. These limitations highlight the need for explanation frameworks that validate reasoning in executable and structured forms and enable modeling of shared reasoning structures.

## 3 Methodology

### 3.1 Executable Explanations for Single-Instance Reasoning

To systematically characterize the local reasoning behavior of large language models (LLMs), we begin by studying *trustworthy explanations* at the level of single inference instances. Existing Chain-of-Thought (CoT) based methods are able to generate fluent reasoning traces; however, such traces do not necessarily reflect the model’s true decision mechanism and often function as post-hoc rationalizations. In contrast, we redefine explanations as *executable reasoning specifications*, whose validity can be verified through external execution. The framework of the executable explanations is illustrated in Figure 1 .

**Definition 1 (Executable Explanation).** Given an input problem  $x$ , an executable explanation is defined as a structured sequence of reasoning steps

$$E = (e_1, e_2, \dots, e_T), \tag{1}$$

where each step  $e_t$  specifies an executable operation, including its associated symbolic variables and a brief natural language description. The explanation is treated as a process specification rather than a narrative account; therefore, it is not allowed to explicitly reveal intermediate numerical values or the final answer.

In practice, we prompt the LLM to generate candidate explanations using fixed prompting strategies (e.g., CoT, Plan-and-Solve). All generated reasoning traces are uniformly treated as executable explanations instead of purely descriptive text.

**Definition 2 (Trustworthy Explanation).** An executable explanation  $E$  is considered *trustworthy* if it contains sufficient information such that an independent executor can recover the correct answer without access to the original input problem  $x$ .

To evaluate whether a generated explanation satisfies this criterion, we introduce a *blind execution verifier*  $V$ , whose role is to translate textual explanations into an executable domain and execute them sequentially. To prevent the verifier from introducing external knowledge beyond the explanation itself, we construct a composite verification framework that integrates LLM-based step interpretation with white-box components such as arithmetic solvers and rule-based matchers. In this framework, the LLM is only responsible for interpreting and executing the provided steps, while the white-box modules ensure the correctness of each operation.

The verifier receives only the explanation sequence  $E$ , without access to the original problem  $x$ , and produces a predicted answer:

$$\hat{y} = V(E). \quad (2)$$

If blind execution successfully yields the correct answer, the explanation is deemed to encode a complete and executable solution structure. This indicates that the original LLM is capable of generating executable reasoning processes that lead to correct solutions under the given input, and the explanation is considered trustworthy.

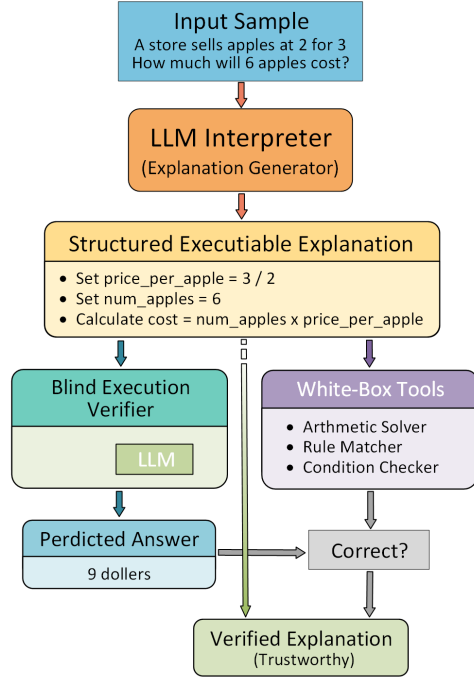


Figure 1: Generation and verification of executable explanations. Given an input instance, the LLM interpreter produces a structured executable explanation consisting of explicit reasoning steps. The explanation is executed by a blind execution verifier to obtain a predicted answer, while white-box tools independently verify the correctness of each reasoning step.

### 3.2 Local Feasible-Region Modeling via Structure-Preserving Perturbations

While executable explanations for a single instance can verify whether a reasoning trace encodes a valid solution structure, they do not characterize the model’s behavioral stability under nearby input variations. In practical deployments, one often cares not only about whether the model succeeds on a specific sample, but also whether it preserves correct decisions under small perturbations, or whether seemingly similar inputs can trigger unexpected failures. To address this limitation, we propose a *local feasible-region modeling* framework that characterizes the feasible reasoning structure in the neighborhood input space, thereby providing a foundation for stability and robustness assessment. Figure 2 illustrates the construction process of the executable feasible-region DAG.

**Structure-Preserving Perturbation Generation.** Given a target instance  $x$ , the LLM first identifies perturbable factors and modifies them *without changing the overall solution structure*, producing a neighborhood set of perturbed instances:

$$\mathcal{N}(x) = \{x^{(0)}, x^{(1)}, \dots, x^{(K)}\}, \quad (3)$$

where  $x^{(0)}$  denotes the original instance. Each perturbed instance is constructed following predefined perturbation types, such as parameter variations, entity substitutions, or condition adjustments. Given the labels of the original instance (including the reference solution procedure and the correct answer), we obtain the corresponding labels for perturbed instances by combining LLM-based reasoning with white-box tools (e.g., a numerical calculator) for verification.

**Reasoning Behavior Evaluation on Perturbations.** We apply the LLM to each instance in  $\mathcal{N}(x)$  to obtain its reasoning steps and predicted answer. For a reasoning step  $s_i$ , we quantify (i) *semantic correctness* and (ii) *blind executability*.

(i) *Semantic correctness.* Let  $C_i \in \{0, 1\}$  denote the semantic consistency indicator for the  $i$ -th reasoning step. Specifically,  $C_i$  is determined by a LLM semantic verifier  $g(s_i, s_i^{\text{ref}})$  that evaluates whether the generated step  $s_i$  is semantically consistent with the corresponding reference step  $s_i^{\text{ref}}$ :

$$C_i = \begin{cases} 1, & \text{if } g(s_i, s_i^{\text{ref}}) = 1, \\ 0, & \text{otherwise.} \end{cases} \quad (4)$$

(ii) *Blind executability.* Let  $n_i^{\text{exec}}$  denote the number of perturbed instances in  $\mathcal{N}(x)$  for which step  $s_i$  can be executed successfully by the verifier. The execution success rate is defined as

$$R_i = \frac{n_i^{\text{exec}}}{|\mathcal{N}(x)|}. \quad (5)$$

Finally, we define the step reliability weight as

$$W_i = C_i \cdot R_i, \quad (6)$$

which jointly captures semantic correctness and robustness to local perturbations.

### Local Feasible-Region Graph Construction.

Using all reasoning trajectories observed on the original instance and its neighborhood, we construct a directed acyclic graph (DAG) to represent the local feasible reasoning space. Each node corresponds to a merged reasoning step  $S_i$  and is assigned a weight  $W_i \in [0, 1]$ , while directed edges encode step dependency relations observed across different trajectories. Formally, we represent the graph as

$$G = (S, E). \quad (7)$$

This graph provides a structured and interpretable representation of the reasoning paths that the LLM may exhibit for inputs similar to the original instance, along with their associated correctness and execution success likelihoods, thereby facilitating the analysis of local decision behavior.

### 3.3 Cluster-Level Failure Mode Analysis

Although local feasible region modeling characterizes reasoning stability within the neighborhood of individual samples, its scope remains limited to local behaviors and does not directly reveal class-level failure mechanisms. To address this limitation, we introduce a cluster-level failure mode analysis module that automatically discovers recurring reasoning deficiencies within a problem class and quantifies their influence on prediction outcomes, as illustrated in Figure 3. This enables evaluation of how well the model has internalized the reasoning structure represented by the cluster and facilitates identification of conditions that lead to systematic failures.

**Failure Mode Discovery.** We first partition the dataset into a set of small-scale clusters based on similarity in solution patterns. Clustering is performed through an LLM-assisted inductive summarization process, where each cluster contains  $n$  samples exhibiting comparable reasoning structures. Formally, a sample cluster is defined as:

$$C = \{x_1, x_2, \dots, x_n\}. \quad (8)$$

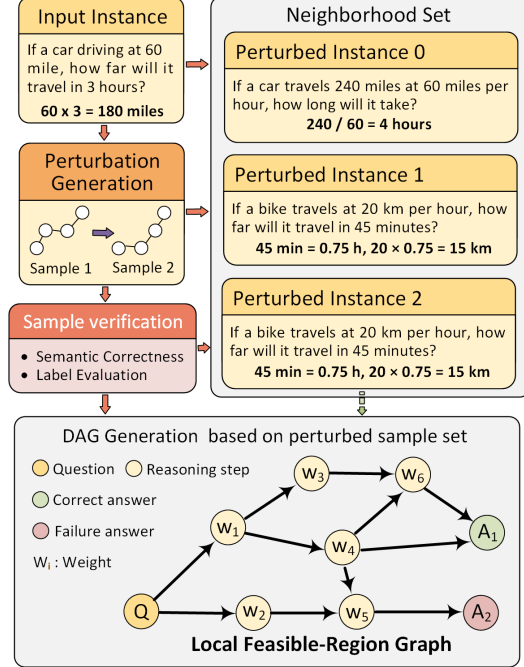


Figure 2: Construction of the local feasible-region graph via structure-preserving perturbations. Verified perturbed samples are aggregated into a directed acyclic graph, where nodes represent reasoning steps and edges encode their dependencies.

Given a cluster  $C$  and a reasoning trace  $E$ , we define a failure mode as a minimal structural condition whose presence increases the likelihood of incorrect prediction. Each failure mode is represented as a binary indicator:

$$f_i : (x, E) \rightarrow \{0, 1\}, \quad (9)$$

where  $f_i = 1$  indicates that the corresponding failure condition is detected in the input or reasoning process. To ensure operational validity, each failure mode must be identifiable from the reasoning trace or input structure, manipulable through controlled perturbations, and locally minimal with respect to its influence.

Failure modes are automatically extracted using an LLM-driven analysis procedure. For incorrectly predicted samples, the generated reasoning traces are aligned with reference solution procedures to identify divergent steps. The LLM then abstracts each discrepancy into candidate failure descriptions that include the affected reasoning components, the associated input fragments, and the hypothesized cause of error. Candidate descriptions across samples are subsequently normalized and merged via semantic clustering to obtain a compact failure mode set:

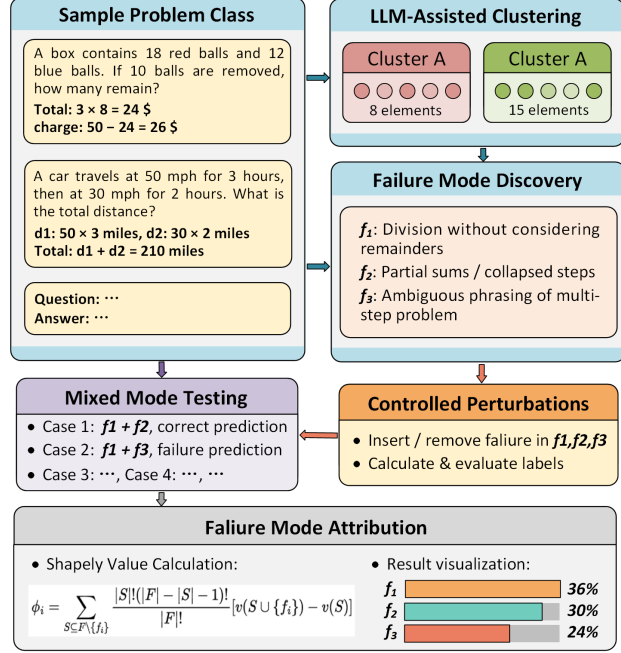


Figure 3: Overview of the proposed failure mode discovery and attribution framework. Given a sample problem class, semantically similar instances are grouped via LLM-assisted clustering, followed by systematic failure mode discovery. Controlled perturbations and mixed-mode testing are then performed to evaluate reasoning behavior under failure combinations. Finally, Shapley value attribution quantifies the causal impact of each failure mode on prediction outcomes.

$$F = \{f_1, f_2, \dots, f_K\}. \quad (10)$$

This process yields a structured library of recurring failure conditions specific to the cluster.

**Failure Importance Estimation.** To quantify the influence of each failure mode on reasoning outcomes, we construct counterfactual instances through controlled perturbations. Specifically, selected failure modes are injected into correctly solved samples, while corresponding conditions are removed or simplified for incorrectly solved samples. For perturbed instances whose problem parameters change, ground-truth labels are recomputed using the reference solution procedure. The perturbed samples are then merged with the original cluster to form an augmented cluster  $C'$ .

We evaluate the target LLM on all samples in  $C'$  and measure prediction correctness under different failure configurations. The contribution of each failure mode is estimated using Shapley value attribution. Let  $F = \{f_1, \dots, f_K\}$  denote the failure mode set. The Shapley value for failure mode  $f_i$  is computed as:

$$\phi_i = \sum_{S \subseteq F \setminus \{f_i\}} \frac{|S|!(|F| - |S| - 1)!}{|F|!} [v(S \cup \{f_i\}) - v(S)] \quad (11)$$

where  $v(S)$  denotes prediction correctness under configuration  $S$ . The resulting  $\phi_i$  quantifies the marginal impact of each failure mode on prediction errors under controlled perturbations.

The estimated importance values are visualized as a cluster-level failure profile, highlighting dominant error sources and their relative influence. This representation provides an interpretable characterization of the model’s reasoning robustness within the target problem class.

## 4 Experiments

### 4.1 Executable Explanation Reliability Evaluation

We experimentally validate the proposed single-instance executable explanation framework (see Section 3.1 for methodological details). For each input, the reasoning trace generated by the LLM is transformed into a structured sequence of executable steps. We then introduce an independent blind executor that attempts to recover the final answer using only the generated explanation steps, without access to the original problem statement. This protocol explicitly decouples the informational content of the reasoning trace from the original input, allowing us to directly test whether the explanation itself encodes a structurally complete and operational solution procedure.

**Benchmarks.** To comprehensively evaluate explanation reliability and executability, we conduct experiments on multiple representative reasoning benchmarks.

For mathematical reasoning, we employ **GSM8K** Cobbe et al. [2021] and **MATH** Hendrycks et al. [2021], which assess multi-step numerical computation and high-complexity symbolic reasoning. For logical and knowledge-intensive reasoning, we use the multiple-choice subset of **BBH** Suzgun et al. [2023] and the **MMLU-CF** Zhao et al. [2025] dataset, which evaluate formal logical judgment and cross-domain knowledge application, respectively. These datasets span diverse reasoning depths and structural complexities, enabling a comprehensive evaluation across heterogeneous task types.

Due to the computational cost of explanation generation, blind execution, and step-level evaluation, we construct evaluation subsets by randomly sampling 300 instances from the test split of each dataset using a fixed random seed. For datasets with heterogeneous difficulty distributions, we further verify that the sampled subset covers different difficulty levels and reasoning patterns to reduce bias.

**Experimental Settings.** We first evaluate the performance of different reasoning strategies under the proposed executable explanation paradigm. Specifically, we adopt GPT-4o-mini as the base language model and generate explanations using several representative reasoning strategies, including standard Chain-of-Thought (CoT), Zero-Shot CoT, Self-Refine, and Plan-and-Solve prompting. This experiment enables us to analyze the impact of reasoning strategies on explanation executability and structural completeness.

We further investigate the influence of the underlying base model on executable explanation performance. In this experiment, we fix the reasoning strategy to standard CoT prompting and vary the base model under a controlled experimental setting. We evaluate multiple representative model APIs, including GPT-4o-mini, GPT-4.1-nano, and GPT-5-nano, which span different capability levels. This setting allows us to isolate the effect of base model capability on the quality and executability of generated explanations.

To ensure fair comparison, all reasoning strategies and base models use the same prompt template and generation protocol, and are constrained to produce structured step-level reasoning without explicitly revealing intermediate numerical values or final answers. During the blind execution stage, GPT-4o-mini is uniformly used as the executor to control execution variance across models, ensuring that performance differences reflect explanation quality rather than executor capability.

**Evaluation Metrics.** To systematically quantify explanation reliability, we adopt the Executable Explanation Evaluation ( $E^3$ ) framework. Let  $N$  denote the total number of evaluation samples. We define four outcome statistics:  $N_{\text{exec}}$ ,  $N_{\text{orig}}$ ,  $N_{\text{joint}}$ , and  $N_{\text{rec}}$ , representing the numbers of samples correctly solved by the blind executor, by the original reasoning method, by both, and only through executable recovery, respectively.

We measure overall executability and baseline performance using:

$$EA = \frac{N_{\text{exec}}}{N}, \quad OA = \frac{N_{\text{orig}}}{N}. \quad (12)$$

Executable Accuracy (EA) reflects the proportion of instances for which the explanation alone contains sufficient procedural information to recover the correct answer, while Original Accuracy (OA) corresponds to the standard prediction accuracy of the original reasoning method.

Table 1: Executable Explanation Evaluation Results on Four Benchmarks (%).

Method	MATH				MMLU			
	EA	OA	EC	ERR	EA	OA	EC	ERR
CoT	68.0	74.0	91.9	0.0	66.0	68.0	97.1	0.0
Self-Refine	80.0	82.0	97.6	0.0	54.0	62.0	87.1	0.0
Zero-Shot-CoT	70.0	76.0	92.1	0.0	62.0	70.0	74.3	33.3
Plan-and-Solve	60.0	72.0	80.6	7.1	66.0	70.0	88.6	13.3
<b>Avg.</b>	69.5	76.0	90.6	1.8	62.0	67.5	86.8	11.7

Method	GSM8K				BBH			
	EA	OA	EC	ERR	EA	OA	EC	ERR
CoT	88.0	92.0	95.7	0.0	62.0	68.0	88.2	6.3
Self-Refine	92.0	92.0	100.0	0.0	54.0	64.0	75.0	16.7
Zero-Shot-CoT	92.0	96.0	95.8	0.0	52.0	68.0	73.5	6.3
Plan-and-Solve	94.0	96.0	97.9	0.0	38.0	64.0	56.2	5.6
<b>Avg.</b>	91.5	94.0	97.4	0.0	51.5	66.0	73.2	8.7

To evaluate explanation trustworthiness under blind execution, we compute Executable Consistency:

$$EC = \frac{N_{\text{joint}}}{N_{\text{orig}}}. \quad (13)$$

This metric quantifies the proportion of originally correct predictions whose reasoning traces remain executable when the problem statement is removed.

We further assess the recovery capability of executable explanations using Executable Recovery Rate:

$$ERR = \frac{N_{\text{rec}}}{N - N_{\text{orig}}}. \quad (14)$$

This metric measures the fraction of originally incorrect instances for which the executor is able to recover the correct answer solely based on the explanation steps.

**Results.** Table 1 reports the executable explanation evaluation results for different reasoning strategies under a fixed base model across four benchmarks.

First, on numerical reasoning datasets (GSM8K and MATH), Executable Accuracy (EA) closely tracks Original Accuracy (OA). For example, on GSM8K, Plan-and-Solve achieves EA/OA of 94.0%/96.0%, while Zero-Shot CoT reaches 92.0%/96.0%. The gap remains within a few percentage points across methods. Executable Consistency (EC) is also high: Self-Refine attains 100.0% EC on GSM8K, and 97.6% on MATH. These results indicate that, for numerical tasks, explanations that lead to correct answers typically encode sufficiently complete procedural structures to remain executable even when the problem statement is removed.

In contrast, on knowledge- and logic-intensive tasks (MMLU and BBH), EA degrades more noticeably relative to OA. For instance, on BBH, Plan-and-Solve obtains an OA of 64.0% but an EA of only 38.0%, with EC dropping to 56.2%. A similar trend appears on MMLU, where Zero-Shot CoT shows EA/OA of 62.0%/70.0%. These discrepancies suggest that, in tasks, explanations may rely on implicit information from the original input rather than forming fully self-contained procedures.

Executable Recovery Rate (ERR) exhibits a distinct pattern and warrants separate discussion. In most numerical settings (e.g., GSM8K), ERR remains at 0.0%, indicating that blind execution rarely corrects originally incorrect predictions. However, on MMLU-CF, Zero-Shot CoT reaches an ERR of 33.3%, and on BBH, Self-Refine achieves 16.7%. This suggests that, in certain multiple-choice reasoning scenarios, explanation structures occasionally contain recoverable signals that allow the executor to correct errors made by the original inference.

Overall, numerical datasets exhibit consistently high EC (97.4% on GSM8K and 90.6% on MATH on average), while multiple-choice benchmarks show substantially lower EC (86.8% on MMLU

Table 2: Executable Explanation Evaluation across Different Model APIs on MATH and MMLU Datasets (CoT Method). EA: Executable Accuracy; OA: Original Accuracy; EC: Execution Consistency; ERR: Execution Error Rate.

Model	MATH Dataset				MMLU Dataset			
	EA	OA	EC	ERR	EA	OA	EC	ERR
gpt-4o-mini	68.0	74.0	91.9	0.0	66.0	68.0	97.1	0.0
gpt-4.1-nano	68.0	72.0	91.7	7.1	58.0	64.0	84.4	11.1
gpt-5-nano	88.0	92.0	95.7	0.0	70.0	70.0	100.0	0.0

and 73.2% on BBH). These findings indicate that executable explanation reliability is strongly task-dependent, and that logical or knowledge-intensive tasks pose greater challenges for generating fully self-contained procedural reasoning.

Table 2 reports the executable explanation evaluation results across different base models under a fixed CoT prompting strategy. Overall, we observe a consistent trend that stronger base models produce explanations with higher executability and structural completeness.

On the MATH dataset, GPT-5-nano achieves substantially higher executable accuracy than GPT-4o-mini and GPT-4.1-nano (88.0%, 68.0%, and 68.0%, respectively). A similar trend is observed on MMLU, where GPT-5-nano attains the highest executable accuracy (70.0%), while GPT-4.1-nano exhibits lower executability (58.0%). Furthermore, execution consistency (EC) also improves with model capability. For example, GPT-5-nano achieves perfect execution consistency (100.0%) on MMLU, whereas weaker models show lower consistency and higher execution error rates.

These results indicate that executable explanation quality is strongly correlated with base model capability. More capable models are more likely to generate structurally complete and executable reasoning processes, further validating the generality of the proposed executable explanation verification framework across different model capability levels.

## 4.2 Structural Validity Evaluation of Local Feasible Regions

To evaluate whether the proposed local feasible-region representation constructed from structure-preserving perturbations around a single anchor instance can capture representative decision structures shared by a problem class, we conduct experiments on sample clusters  $C = \{x_1, \dots, x_n\}$ . The goal is not to build a standalone predictor, but to quantitatively assess whether the constructed feasible-region DAG contains sufficient structural information to characterize the LLM’s reasoning behavior on semantically similar instances. In addition, we further evaluate whether the perturbation-induced DAG can adequately cover reasoning trajectories observed across different instances within the same cluster, thereby validating its structural representational capability.

**Experimental Setup.** Our experiments are conducted on the MATH and MMLU-CF datasets. We identify semantically similar samples using a combination of LLM-assisted grouping and manual selection, and construct five sample clusters per dataset, each containing 10–20 instances. For each cluster, we select a representative anchor instance and generate a set of structure-preserving perturbations. Reference solutions for perturbed instances are derived from the known solution procedure and verified using external tools (e.g., numerical calculators). We then aggregate reasoning traces from the original and perturbed instances using the proposed framework to construct a local feasible-region DAG, where nodes represent merged reasoning steps and edges encode step dependency relations observed across trajectories.

We evaluate reasoning behavior from two complementary perspectives. First, for success-rate prediction, we generate Chain-of-Thought (CoT) reasoning traces for all instances in the cluster. A separate LLM is provided with the problem statement, the constructed feasible-region DAG, and the generated reasoning trace, and asked to predict the probability of execution success. Prediction quality is evaluated using cross-entropy loss across all instances in the cluster. We compare the proposed perturbation-guided structural representation with a baseline of equal computational budget. In this baseline, instead of constructing a DAG from perturbations, we perform repeated CoT sampling

Table 3: Success Rate Prediction Results on MATH and MMLU-CF. Lower CE indicates better calibration.  $\Delta\text{CE} = \text{Baseline CE} - \text{DAG CE}$ .

Category	Pert. SR	Test SR	DAG CE↓	Baseline CE↓	$\Delta\text{CE}$
<b>MATH</b>					
Prealgebra	50.0%	87.5%	<b>1.05</b>	11.51	+10.46
Number Theory	83.3%	75.0%	<b>0.75</b>	1.39	+0.64
Intermediate Alg.	33.3%	50.0%	<b>0.30</b>	0.75	+0.45
Counting & Prob.	50.0%	75.0%	<b>1.72</b>	8.69	+6.97
Precalculus	16.7%	37.5%	<b>0.43</b>	0.79	+0.36
<i>Average</i>	46.7%	65.0%	<b>0.85</b>	4.63	+3.78
<b>MMLU-CF</b>					
Classification and Rules	83.3%	65.0%	1.00	<b>0.83</b>	-0.17
Health and Medicine	100.0%	80.0%	<b>0.53</b>	4.51	+3.98
History and Politics	66.6%	75.0%	<b>0.67</b>	4.51	+3.84
Science and Technology	83.3%	65.0%	0.98	<b>0.83</b>	-0.15
Economics and Finance	100.0%	40.0%	<b>1.69</b>	13.82	+12.13
<i>Average</i>	86.6%	65.0%	<b>0.97</b>	4.90	+3.93

on the anchor instance and encode the resulting reasoning traces as a DAG-style auxiliary input containing only reasoning paths derived from the anchor instance.

Second, to evaluate structural coverage, we perform step-level alignment between reasoning trajectories and the constructed feasible-region DAG. For each instance, reasoning steps are matched to DAG nodes based on semantic equivalence criteria, and the trajectory coverage ratio is computed as the fraction of matched steps. We conduct this evaluation under three perturbation regimes: mild, moderate, and aggressive. These regimes differ in the magnitude of input modifications while preserving the underlying solution structure.

**Evaluation Metrics.** In the first experiment, prediction quality is measured using cross-entropy (CE) between the predicted success probability and the ground-truth execution outcome, reported as Pret. CE and Baseline CE. We also report the average execution success rate for perturbation-induced clusters and original test clusters, denoted as Pret. SR and Test SR, respectively.

In the second experiment, we report the average trajectory coverage ratio across all instances and their perturbation neighborhoods, denoted as GT Match and Pret Match. These metrics quantify the extent to which the constructed feasible-region DAG captures reasoning trajectories generated by the model and present in the reference solutions. In addition, we report statistics of the DAG, including the number of nodes and edges, to characterize complexity of the feasible-region representation.

**Results.** Table 3 presents the success rate prediction performance of the proposed DAG-based predictor and the baseline CoT-based predictor on the MATH and MMLU-CF datasets.

Compared with the baseline predictor, the proposed DAG-based predictor achieves substantially lower cross-entropy (CE) across most categories and datasets. On the MATH dataset, the average CE is reduced from 4.63 to 0.85, corresponding to an absolute reduction of 3.78 and a relative reduction of approximately 81.6%. This improvement is particularly pronounced in categories such as Prealgebra and Counting & Probability, with CE reductions of +10.46 and +6.97, respectively. These results indicate that the feasible-region DAG constructed from structure-preserving perturbations effectively captures dependencies between reasoning steps and enables reliable success probability estimation for semantically similar problems.

A similar trend is observed on the MMLU-CF dataset. The proposed method reduces the average CE from 4.90 to 0.97, achieving an absolute reduction of 3.93. Substantial improvements are observed in knowledge-intensive domains such as Economics and Finance and Health and Medicine. In addition, the perturbation success rate (Pert. SR) is generally close to the true success rate on the sample

Table 4: DAG trajectory coverage results on MATH and MMLU-CF datasets. Nodes and Edges denote the size of the feasible-region DAG. Pret.(%) represents the average trajectory coverage rate of perturbed instances, while GT(%) denotes the coverage rate of ground-truth reasoning trajectories.

Perturbation	MATH Dataset				MMLU-CF Dataset			
	Nodes	Edges	Pret.(%)	GT(%)	Nodes	Edges	Pret.(%)	GT(%)
Mild	9	35	51.9	34.8	18	29	50.8	48.3
Moderate	10	35	74.2	62.9	23	30	58.8	53.1
Aggressive	13	31	96.4	96.4	26	32	66.6	61.3

cluster (Test SR), indicating that the generated perturbations effectively model the underlying data distribution and support the validity of the feasible-region representation.

Overall, these results demonstrate that providing the feasible-region DAG as auxiliary structural information significantly improves the LLM’s ability to predict reasoning success probability and confirms that the constructed representation contains sufficient structural information to characterize cluster-level reasoning behavior.

Table 4 reports the trajectory coverage of the constructed feasible-region DAG under different perturbation regimes. On MATH, trajectory coverage increases substantially as perturbation strength increases. Under aggressive perturbations, both Pret.(%) and GT(%) reach 96.4%, indicating that the constructed DAG captures nearly all reasoning steps observed across both perturbed and original instances. This suggests that larger perturbation diversity enables the feasible-region representation to more completely characterize the underlying reasoning structure in mathematical reasoning tasks.

On MMLU-CF, a similar but more moderate trend is observed. Pret.(%) increases from 50.8% under mild perturbations to 66.6% under aggressive perturbations, while GT(%) improves from 48.3% to 61.3%. The lower overall coverage compared to GSM8K reflects the greater structural variability and ambiguity of reasoning patterns in knowledge-intensive tasks.

Overall, these results demonstrate that the perturbation-constructed feasible-region DAG provides substantial structural coverage of both perturbed and ground-truth reasoning trajectories, supporting its effectiveness as a compact representation of the local reasoning space.

### 4.3 Cluster-Level Failure Mode Evaluation

This experiment aims to validate the effectiveness of the proposed neighborhood-based failure-mode explanation framework. Specifically, we first identify semantically and structurally similar samples from the dataset and group them into clusters. For each cluster, we discover candidate failure modes and quantify their causal contributions to prediction outcomes. Furthermore, to evaluate the robustness of the failure-mode discovery process under limited sample conditions, we conduct a subsampling stability analysis to examine whether the identified failure modes and their causal importance rankings remain consistent as the number of available samples varies.

**Experimental Setup.** We conduct experiments on two benchmark datasets: GSM8K for mathematical reasoning and the multiple-choice subset of BBH for logical reasoning. For each dataset, we use a GPT-4o-mini–assisted inductive summarization procedure to construct two representative clusters corresponding to distinct problem types. Based on each cluster, we construct a candidate failure-mode set and select five failure modes that are assessed by the LLM as having high structural impact potential, i.e., most likely to influence reasoning outcomes when injected or removed.

We then generate counterfactual variants through controlled interventions on cluster instances, including: (a) injecting failure conditions into originally correctly predicted instances, and (b) removing or simplifying failure conditions from originally incorrectly predicted instances. When an intervention modifies the underlying problem parameters or structure, the ground-truth label is recomputed using the reference solution procedure to ensure label correctness.

Using the original and intervened samples, we construct an evaluation set. We evaluate the target model (GPT-4o-mini) on these samples and compute the empirical prediction correctness, which defines the characteristic function  $v(S)$ . Based on this function, we compute the Shapley value of

Table 5: Cluster-Level Failure Mode Analysis on GSM8K and BBH (Enhanced Shapley Values).

Failure Mode	Error Type	Complexity	Shapley $\phi$	Impact
<b>GSM8K – Multi-step Arithmetic (Acc: 83.3%)</b>				
Percentage Confusion	Calculation	High	0.22	Med.
Multi-step Calculations	Multi-step	High	0.17	Low
Unit Conversion Errors	Logic	Medium	0.11	Low
<b>GSM8K – Word Problems with Ratios (Acc: 91.7%)</b>				
Complex Financial Calculations	Calculation	High	0.27	Med.
Misinterpretation of Percentages	Comprehension	Medium	0.21	Med.
Sequential Calculation Errors	Multi-step	High	0.13	Low
<b>BBH – Logical Reasoning (Acc: 83.3%)</b>				
Data Interpretation	Inference	Medium	0.29	Med.
Order of Objects	Constraint	High	0.21	Med.
Adjective Order	Comprehension	Medium	0.13	Low
<b>BBH – Spatial-Temporal Reasoning (Acc: 75.0%)</b>				
Date Calculation Errors	Logic	High	0.35	High
Item Count Misjudgment	Logic	Low	0.35	High
Context Misinterpretation	Comprehension	Medium	0.02	Low

each failure mode according to Equation 11 and rank failure modes accordingly. This process enables identification of the dominant structural weaknesses responsible for systematic prediction failures within each problem class.

To further assess stability, we perform subsampling analysis on each cluster. Specifically, we construct subsampled clusters with varying sizes

$$n \in \{5, 10, 20, 40\}.$$

For each subsampled cluster, we repeat the complete failure-mode discovery and Shapley value estimation process. Stability is evaluated by comparing the discovered failure-mode sets and their causal importance rankings across different subsampling scales, thereby assessing the robustness of the proposed method under limited sample availability.

**Evaluation Metrics.** For causal contribution analysis, we use the Shapley value as the quantitative measure of each failure mode’s causal impact on prediction outcomes. The formal definition follows Equation 11.

For stability analysis, we use two metrics to quantify consistency across different subsampling scales. The Jaccard similarity measures the overlap between Top- $k$  failure-mode sets discovered under different subsampling conditions:

$$\text{Jaccard} = \frac{|F_a \cap F_b|}{|F_a \cup F_b|}. \tag{15}$$

Higher Jaccard similarity indicates greater consistency in failure-mode discovery.

The Kendall correlation coefficient ( $\tau$ ) measures the consistency of failure-mode importance rankings:

$$\tau = \frac{C - D}{\frac{1}{2}k(k - 1)}, \tag{16}$$

where  $C$  and  $D$  denote the numbers of concordant and discordant failure-mode pairs, respectively.

Higher Kendall  $\tau$  indicates more stable causal importance rankings across different sample sizes.

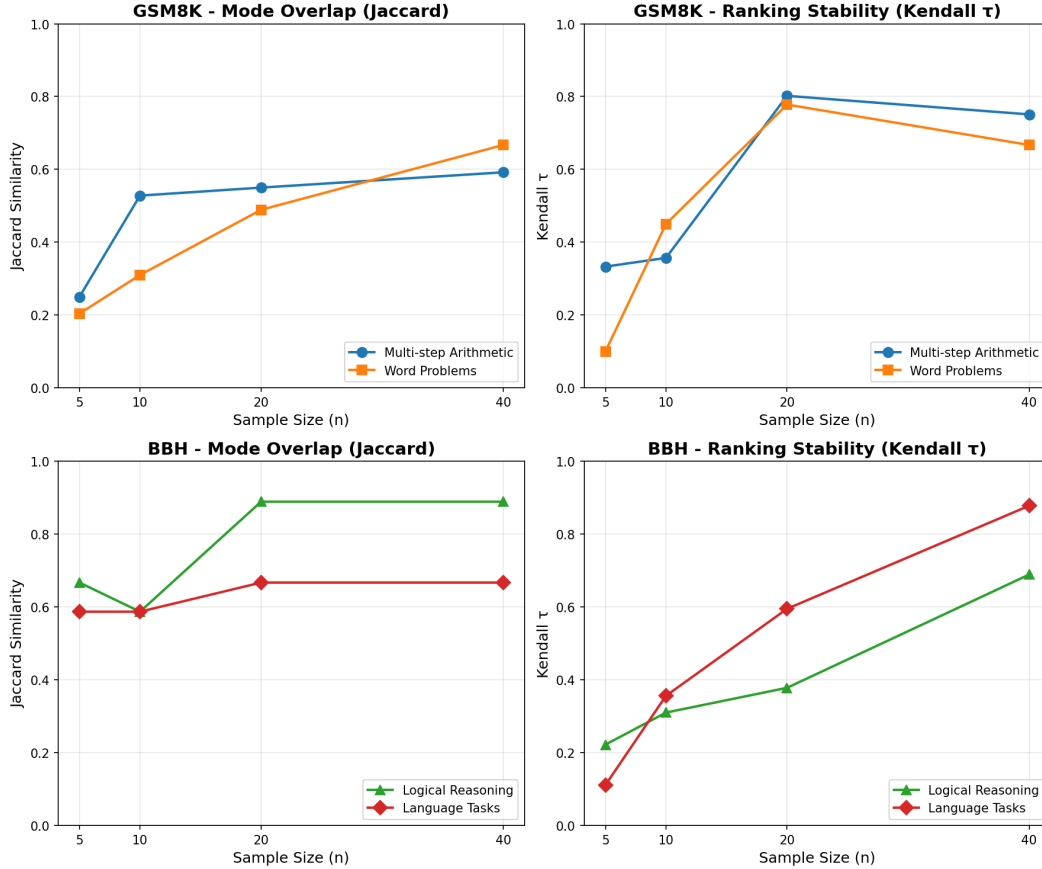


Figure 4: Cluster size scaling of failure mode stability. Mode overlap (Jaccard) and ranking stability (Kendall's  $\tau$ ) increase and saturate with cluster size, indicating robust failure mode discovery.

**Results.** Table 5 presents the cluster-level failure mode analysis results on the GSM8K and BBH datasets. Overall, LLM reasoning failures are not uniformly distributed but are concentrated in specific structural reasoning patterns.

On GSM8K, in the Multi-step Arithmetic cluster, Percentage Confusion exhibits the highest impact ( $\phi = 0.22$ ). In the Word Problems with Ratios cluster, Complex Financial Calculations ( $\phi = 0.27$ ) and Misinterpretation of Percentages ( $\phi = 0.21$ ) contribute substantially to prediction failure. These findings indicate that failures are strongly associated with complex numerical transformations and multi-stage quantitative reasoning.

A similar trend is observed on the BBH dataset. In the Logical Reasoning cluster, Data Interpretation has the highest influence ( $\phi = 0.29$ ). In the Spatial-Temporal Reasoning cluster, Date Calculation Errors and Item Count Misjudgment both exhibit the highest Shapley values ( $\phi = 0.35$ ), indicating that temporal reasoning and state-tracking operations represent critical bottlenecks. In contrast, Context Misinterpretation shows relatively low influence ( $\phi = 0.02$ ), suggesting that general comprehension errors contribute less significantly to overall failure.

These results demonstrate that LLM reasoning failures are primarily driven by specific structural reasoning operations rather than general comprehension limitations. The proposed perturbation-based framework effectively identifies and quantifies the causal impact of failure modes, providing fine-grained cluster-level interpretability and supporting structured analysis of reasoning robustness.

Figure 4 shows the stability curves measured by mode overlap (Jaccard similarity) and ranking stability (Kendall's  $\tau$ ) as a function of sample size. Overall, both metrics improve as cluster size increases, indicating more reliable failure mode identification and causal importance estimation.

On GSM8K, Jaccard similarity increases from 0.25 to 0.59 for Multi-step Arithmetic and from 0.20 to 0.67 for Word Problems as  $n$  increases from 5 to 40. Correspondingly, Kendall's  $\tau$  increases to 0.75

and 0.67, respectively, demonstrating improved ranking consistency. On BBH, stability improves more rapidly. Logical Reasoning reaches a Jaccard similarity of 0.89 by  $n = 20$ , while Language Tasks exhibit steadily increasing ranking stability, reaching  $\tau = 0.88$  at  $n = 40$ .

Notably, both overlap and ranking stability begin to saturate at moderate cluster sizes ( $n \approx 20$ ), indicating that reliable failure mode discovery can be achieved without large numbers of samples. These results demonstrate that the proposed framework provides robust and sample-efficient identification of structural failure patterns.

## 5 Conclusion

In this work, we propose a unified framework for analyzing the reliability and robustness of large language model (LLM) reasoning through executable verification and perturbation-driven structural analysis. We introduce executable explanations as structured reasoning specifications and develop a blind execution verification mechanism to directly assess their operational validity. To characterize local reasoning behavior, we construct perturbation-guided feasible-region DAGs that capture the structural space of valid reasoning trajectories. Furthermore, we propose a cluster-level failure mode analysis framework that automatically discovers recurring structural weaknesses and quantifies their causal impact using Shapley value attribution. Together, these components provide a principled approach for understanding LLM reasoning behavior at both instance and structural levels.

Extensive experiments across multiple reasoning benchmarks demonstrate the effectiveness of the proposed framework. Executable explanations reliably encode complete solution procedures, while the feasible-region DAG provides strong structural coverage of the reasoning space and significantly improves prediction of execution success probability. Cluster-level analysis further reveals that reasoning failures are driven by identifiable structural patterns rather than random errors, and stability experiments confirm that these failure modes can be robustly identified even with limited samples. Overall, this work establishes a new paradigm for interpretable and verifiable LLM reasoning analysis, providing both fine-grained diagnostic capability and a foundation for improving the reliability of LLM-based reasoning systems.

## References

- Tamera Lanham, Anna Chen, Ansh Radhakrishnan, Benoit Steiner, Carson Denison, Danny Hernandez, Dustin Li, Esin Durmus, Evan Hubinger, Jackson Kernion, et al. Measuring faithfulness in chain-of-thought reasoning. *arXiv preprint arXiv:2307.13702*, 2023.
- Debjit Paul, Robert West, Antoine Bosselut, and Boi Faltings. Making reasoning matter: Measuring and improving faithfulness of chain-of-thought reasoning. In *Findings of the Association for Computational Linguistics: EMNLP 2024*, pages 15012–15032, 2024.
- Martin Tutek, Fateme Hashemi Chaleshtori, Ana Marasović, and Yonatan Belinkov. Measuring faithfulness of chains of thought by unlearning reasoning steps. *arXiv e-prints*, pages arXiv–2502, 2025.
- Chirag Agarwal, Sree Harsha Tanneru, and Himabindu Lakkaraju. Faithfulness vs. plausibility: On the (un) reliability of explanations from large language models. *arXiv preprint arXiv:2402.04614*, 2024.
- Vojtech Cahlik, Rodrigo Alves, and Pavel Kordik. Reasoning-grounded natural language explanations for language models. In *World Conference on Explainable Artificial Intelligence*, pages 3–18. Springer, 2025.
- Miles Turpin, Julian Michael, Ethan Perez, and Samuel Bowman. Language models don’t always say what they think: Unfaithful explanations in chain-of-thought prompting. *Advances in Neural Information Processing Systems*, 36:74952–74965, 2023.
- Fazl Barez, Tung-Yu Wu, Iván Arcuschin, Michael Lan, Vincent Wang, Noah Siegel, Nicolas Collignon, Clement Neo, Isabelle Lee, Alasdair Paren, et al. Chain-of-thought is not explainability. *Preprint, alphaXiv*, page v1, 2025.

- Marco Tulio Ribeiro, Sameer Singh, and Carlos Guestrin. "why should i trust you?" explaining the predictions of any classifier. In *Proceedings of the 22nd ACM SIGKDD international conference on knowledge discovery and data mining*, pages 1135–1144, 2016.
- Mohammad Reza Ghasemi Madani, Aryo Pradipta Gema, Gabriele Sarti, Yu Zhao, Pasquale Minervini, and Andrea Passerini. Noiser: Bounded input perturbations for attributing large language models. *arXiv preprint arXiv:2504.02911*, 2025.
- Francesco Ortu, Zhijing Jin, Diego Doimo, Mrinmaya Sachan, Alberto Cazzaniga, and Bernhard Schölkopf. Competition of mechanisms: Tracing how language models handle facts and counterfactuals. In *Proceedings of the 62nd Annual Meeting of the Association for Computational Linguistics (Volume 1: Long Papers)*, pages 8420–8436, 2024.
- Scott M Lundberg and Su-In Lee. A unified approach to interpreting model predictions. *Advances in neural information processing systems*, 30, 2017.
- Miriam Horovicz and Roni Goldshmidt. Tokenshap: Interpreting large language models with monte carlo shapley value estimation. In *Proceedings of the 1st Workshop on NLP for Science (NLP4Science)*, pages 1–8, 2024.
- Yingtai Xiao, Yuqing Zhu, Sirat Samyoun, Wanrong Zhang, Jiachen T Wang, and Jian Du. Tokenshapley: Token level context attribution with shapley value. In *Findings of the Association for Computational Linguistics: ACL 2025*, pages 3882–3894, 2025.
- Fengyuan Liu, Nikhil Kandpal, and Colin Raffel. Attribot: A bag of tricks for efficiently approximating leave-one-out context attribution. *arXiv preprint arXiv:2411.15102*, 2024.
- Sara Patel, Mingxun Zhou, and Giulia Fanti. Maxshapley: Towards incentive-compatible generative search with fair context attribution. *arXiv preprint arXiv:2512.05958*, 2025.
- Haoru Tan, Sitong Wu, Xiuzhe Wu, Wang Wang, Bo Zhao, Zeke Xie, Gui-Song Xia, and Xiaojuan Qi. Understanding data influence with differential approximation. *arXiv preprint arXiv:2508.14648*, 2025.
- Filip Naudot, Tobias Sundqvist, and Timotheus Kampik. llmshap: A principled approach to llm explainability. *arXiv preprint arXiv:2511.01311*, 2025.
- Jason Wei, Xuezhi Wang, Dale Schuurmans, Maarten Bosma, Fei Xia, Ed Chi, Quoc V Le, Denny Zhou, et al. Chain-of-thought prompting elicits reasoning in large language models. *Advances in neural information processing systems*, 35:24824–24837, 2022.
- Takeshi Kojima, Shixiang Shane Gu, Machel Reid, Yutaka Matsuo, and Yusuke Iwasawa. Large language models are zero-shot reasoners. *Advances in neural information processing systems*, 35: 22199–22213, 2022.
- Lei Wang, Wanyu Xu, Yihuai Lan, Zhiqiang Hu, Yunshi Lan, Roy Ka-Wei Lee, and Ee-Peng Lim. Plan-and-solve prompting: Improving zero-shot chain-of-thought reasoning by large language models. In *Proceedings of the 61st annual meeting of the association for computational linguistics (volume 1: long papers)*, pages 2609–2634, 2023.
- Aman Madaan, Niket Tandon, Prakhar Gupta, Skyler Hallinan, Luyu Gao, Sarah Wiegrefe, Uri Alon, Nouha Dziri, Shrimai Prabhumoye, Yiming Yang, et al. Self-refine: Iterative refinement with self-feedback. *Advances in neural information processing systems*, 36:46534–46594, 2023.
- Xiaochuang Han, Daniel Simig, Todor Mihaylov, Yulia Tsvetkov, Asli Celikyilmaz, and Tianlu Wang. Understanding in-context learning via supportive pretraining data. In *Proceedings of the 61st Annual Meeting of the Association for Computational Linguistics (Volume 1: Long Papers)*, pages 12660–12673, 2023.
- Jerry Wei, Jason Wei, Yi Tay, Dustin Tran, Albert Webson, Yifeng Lu, Xinyun Chen, Hanxiao Liu, Da Huang, Denny Zhou, et al. Larger language models do in-context learning differently. *arXiv preprint arXiv:2303.03846*, 2023.

- Xuezhi Wang, Jason Wei, Dale Schuurmans, Quoc Le, Ed Chi, Sharan Narang, Aakanksha Chowdhery, and Denny Zhou. Self-consistency improves chain of thought reasoning in language models. *arXiv preprint arXiv:2203.11171*, 2022.
- Yung-Sung Chuang, Benjamin Cohen-Wang, Shannon Zejiang Shen, Zhaofeng Wu, Hu Xu, Xi Victoria Lin, James Glass, Shang-Wen Li, and Wen-tau Yih. Selfcite: Self-supervised alignment for context attribution in large language models. *arXiv preprint arXiv:2502.09604*, 2025.
- Aman Madaan, Shuyan Zhou, Uri Alon, Yiming Yang, and Graham Neubig. Language models of code are few-shot commonsense learners. In *Proceedings of the 2022 Conference on Empirical Methods in Natural Language Processing*, pages 1384–1403, 2022.
- Wenxuan Zhou, Sheng Zhang, Hoifung Poon, and Muhao Chen. Context-faithful prompting for large language models. In *Findings of the Association for Computational Linguistics: EMNLP 2023*, pages 14544–14556, 2023.
- Karl Cobbe, Vineet Kosaraju, Mohammad Bavarian, Mark Chen, Heewoo Jun, Lukasz Kaiser, Matthias Plappert, Jerry Tworek, Jacob Hilton, Reiichiro Nakano, et al. Training verifiers to solve math word problems. *arXiv preprint arXiv:2110.14168*, 2021.
- Dan Hendrycks, Collin Burns, Saurav Kadavath, Akul Arora, Steven Basart, Eric Tang, Dawn Song, and Jacob Steinhardt. Measuring mathematical problem solving with the math dataset. *arXiv preprint arXiv:2103.03874*, 2021.
- Mirac Suzgun, Nathan Scales, Nathanael Schärli, Sebastian Gehrmann, Yi Tay, Hyung Won Chung, Aakanksha Chowdhery, Quoc Le, Ed Chi, Denny Zhou, et al. Challenging big-bench tasks and whether chain-of-thought can solve them. In *Findings of the Association for Computational Linguistics: ACL 2023*, pages 13003–13051, 2023.
- Qihao Zhao, Yangyu Huang, Tengchao Lv, Lei Cui, Qinzheng Sun, Shaoguang Mao, Xin Zhang, Ying Xin, Qiufeng Yin, Scarlett Li, et al. Mmlu-cf: A contamination-free multi-task language understanding benchmark. In *Proceedings of the 63rd Annual Meeting of the Association for Computational Linguistics (Volume 1: Long Papers)*, pages 13371–13391, 2025.